International Symposium on Hydraulic Structures

May 17th, 9:40 AM

# An Experimental Study of the Performance of an Ogee-Shaped Vertical Intake: Geometrical Parameters of Cross-Vane Vortex Inhibitor

V. Naderi
vadoud.naderi@mail.mcgill.ca

Susan Gaskin
*McGill University*, susan.gaskin@mcgill.ca

## Recommended Citation

Naderi, V. (2018). An Experimental Study of the Performance of an Ogee-Shaped Vertical Intake: Geometrical Parameters of Cross-Vane Vortex Inhibitor. Daniel Bung, Blake Tullis, 7th IAHR International Symposium on Hydraulic Structures, Aachen, Germany, 15-18 May. doi: 10.15142/T3Q064 (978-0-692-13277-7).

7th International Symposium on Hydraulic Structures Aachen, Germany, 15-18 May 2018
ISBN: 978-0-692-13277-7 DOI: 10.15142/T3Q064

# An Experimental Study of the Performance of an Ogee-Shaped Vertical Intake: Geometrical Parameters of Cross-Vane Vortex Inhibitor

V. Naderi[1], S. Gaskin[2]
[1] *University of Tabriz, Department of Water Science and Engineering (PhD) and McGill University (GRT)*
[2]*McGill University, Department of Civil Engineering and Applied Mechanics, Montreal, Canada*
*E-mail: vadoud.naderi@mail.mcgill.ca*

***Abstract:*** *The occurrence of a vortex at an intake may lead to air-entrainment and reduce the discharge rate through the intake. Entrained air entering the high-speed penstock flow may cause serious damage to either the water conveyance system or the turbines in the hydropower station. As the submergence at the intake decreases, the vortex increases in power. At the critical submergence, the rotational velocity of the vortex reduces the pressure at the centre of the vortex sufficiently to result in a lowering of the water surface and the formation of an air-core that, at the limit, allows air to enter the intake. In this experimental research, the effect on the critical submergence of the intake shape and of geometrical parameters (length, height, mesh solidity and perforation diameter) of a cross-vane vortex inhibitor have been studied. Comparing the experimental results to a vertical pipe intake indicated that the critical submergence is somewhat reduced for an ogee-shape intake at low flow rates, and that the ogee intake with a cross-vane vortex inhibitor significantly reduces the critical submergence, and the reduction increases as Froude number decreases (for Fr = 0.5 to 3.2) with little dependence of the geometry of the cross-vanes (within the parameter range studied).*

***Keywords:*** *Vortex, critical submergence, anti-vortex devices, vertical intake, ogee-shape intake, cross-vane vortex inhibitor.*

## 1. Introduction

Dams are built to create reservoirs for use in hydropower, irrigation, drinking water supply and supply for industrial systems. Intake structures collect and convey the water to an outlet or a hydropower system through a penstock. The hydraulic performance of the intake structure plays an important role in determining the flow rate in the water conveyance systems. Sedimentation, surface waves and vortices can adversely affect the intake performance and may even endanger other parts of the water conveyance system. Vortices forming at the intakes can cause performance problems such as vibrations, air-entrainment and a reduction of the discharge rate of the intakes, thus motivating research on inhibiting intake vortex formation. Critical submergence, $S_C$, is defined as the minimum distance between the free surface and the intake mouth at which air-entrainment does not occur. If the intake submergence, or the head of the water at the intake, is less than $S_C$, it is probable that a strong air-core vortex develops, which may entrain debris and air pockets into the water conveyance system. It is, therefore, critical to maintain a submergence greater than the critical submergence year-round; a more challenging task during the dry season. Thus, prevention of or decrease in vortex formation is sought. A common solution is to use anti-vortex devices or vortex inhibitors to decrease the value of $S_C$. According to the vortex classification of Hecker (1987), vortices can be divided into six different categories (Figure 1) ranging from the swirling of a coherent water surface to a fully developed air-core vortex. Hecker's classifications, VT5 and VT6, are the vortices which can entrain air bubbles and air pockets into the intake structure and therefore occur at submergences greater than critical submergence. Critical submergence occurs at classification VT4. Most of the previous research has considered VT5 as the critical vortex while the critical vortex is defined as the strongest vortex which has no air entrainment.

Previous research on vortices can be divided into two different topics: 1) studies on the vortex structure and hydraulic characteristics of the vortex flow (Rankine (1858), Odgard (1986), Rosenhead (1930), Mih (1990), Levi (1991), Hite & Mih (1994), Chen et al. (2007), Li et al. (2008), Wang et al. (2011a), Suerich-Gulick et al. (2014), Cristofano et al. (2014), Sun and Liu (2015) and Rudolf and Klas (2015)), and 2) discharge specifications, critical submergence and anti-vortex devices in the vortex flows ((Daggett and Keulegan (1974), Jain et al. (1978), Anwar and Amphlett (1980), Gulliver et al. (1986), Yildirim and Kocabas (1995), Borghei and Kabiri Samani (2003), Sarkardeh et al. (2010), Tastan and Yildirim (2010), Wang et al. (2011b), Naderi et al. (2013, 2014), Yang et al. (2014), Tastan (2016), Hashid et al. (2015), Shemsi and Kabiri-Samani (2017) and Gao et al. (2018)).

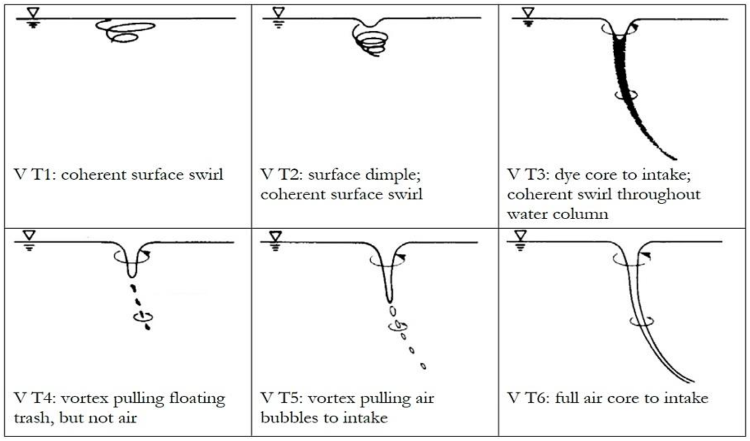

**Figure 1.** Types of vortices.

More general experimental studies using physical models were conducted up to 40 years ago while the majority of recent studies have been undertaken to solve particular prototype problems in hydropower plants or pump stations. Under such conditions, implementing a comprehensive set of experiments can establish some guidelines for design engineers. Table 1 presents selected examples of such guidelines.

**Table 1.** $S_C$ prediction formulas as a function of intake Froude number.

| Researcher | Formula | Comment |
|---|---|---|
| Berge (1966) | $\frac{S_C}{D} = -0.25 + 3.3\sqrt{Fr}$ | D and Fr are intake diameter and Froude number respectively |
| Reddy and Pickford (1972) | $\frac{S_C}{D} = 1 + Fr$ | |
| Rindels and Gulliver (1983) | $\frac{S_C}{D} = 1.7\ Fr$ | Bellmouth intakes only |
| ASCE (1995) | $\frac{S_C}{D} = 1 + 2.3\ Fr$ | When the potential for vortex occurrence is high. |
| Moller (2013) | $\frac{S_C}{D} = 5.3 - 2.5\ Fr^{-0.45}$ | $0.26 \leq Fr \leq 1.2$ |

Naderi (2013) demonstrated that the bell-mouth intake concentrates the vortex as it enters the intake due to a reduction in the intake diameter at lower elevations. Naderi (2014) indicated that combining bell-mouth intakes with vertical anti-vortex plates not only increases the discharge coefficient of the intake but also decreases the critical submergence. Hashid et al. (2015), through experimental studies on horizontal bell-mouth intakes, introduced the ’Sensitivity Parameter’ of intakes that quantifies the increasing sensitivity of the performance of intakes at lower flow rates.

Based on Borghei and Kabiri-Samani (2010) and Naderi (2013 & 2014), anti-vortex devices are essential for eliminating the rotational flow effects on the intake structure and discharge coefficient and for reducing the critical submergence, $S_C$. In this study, an ogee-shaped bell-mouth intake was investigated and chosen due to its acceptable performance at lower discharge rates. A parameter study of the ogee-shaped intake combined with a cross-vane vortex inhibitor, with a range of geometrical parameters (length, height, solidity and perforation diameter of the vanes), was used to determine the optimum combination over a range of flow rates (intake Froude numbers) with the aim of providing basic guidelines for engineering projects.

## 2. Experimental Equipment, Methodology and Dimensional Analysis

Flume experiments of a uniform approach flow to a vertical intake were undertaken in the hydraulics laboratory of the University of Tabriz. The flume consisted of a short straight section 1 m long and 1 m wide followed by a semi-circular end section of 1 m diameter. The vertical intake of 0.4 m height and 70.4 mm diameter ($D$) was placed centrally at the end of the straight section or, equivalently, at the origin of the semi-circular end section as shown in Figure 2. To provide a uniform and steady approach flow, a constant head tank (with an overflow) supplied the flume via a vertical diffuser pipe located behind a 0.1 m thick sand screen and 0.2 m from the upstream end of the flume. The flow into the intake was conveyed to a downstream flume, where the discharge was measured using a V-notch weir. The water depth in the test chamber and just upstream of the V-notch weir (at locations noted in Figure 2) was measured with ultrasonic water level meters at 4 Hz. Side wall and bed friction effects on the vortex flow in the experimental model was negligible due to a clearance of 7D and 6D, respectively (meeting the criteria of > 4D, Anwar et al. 1978).

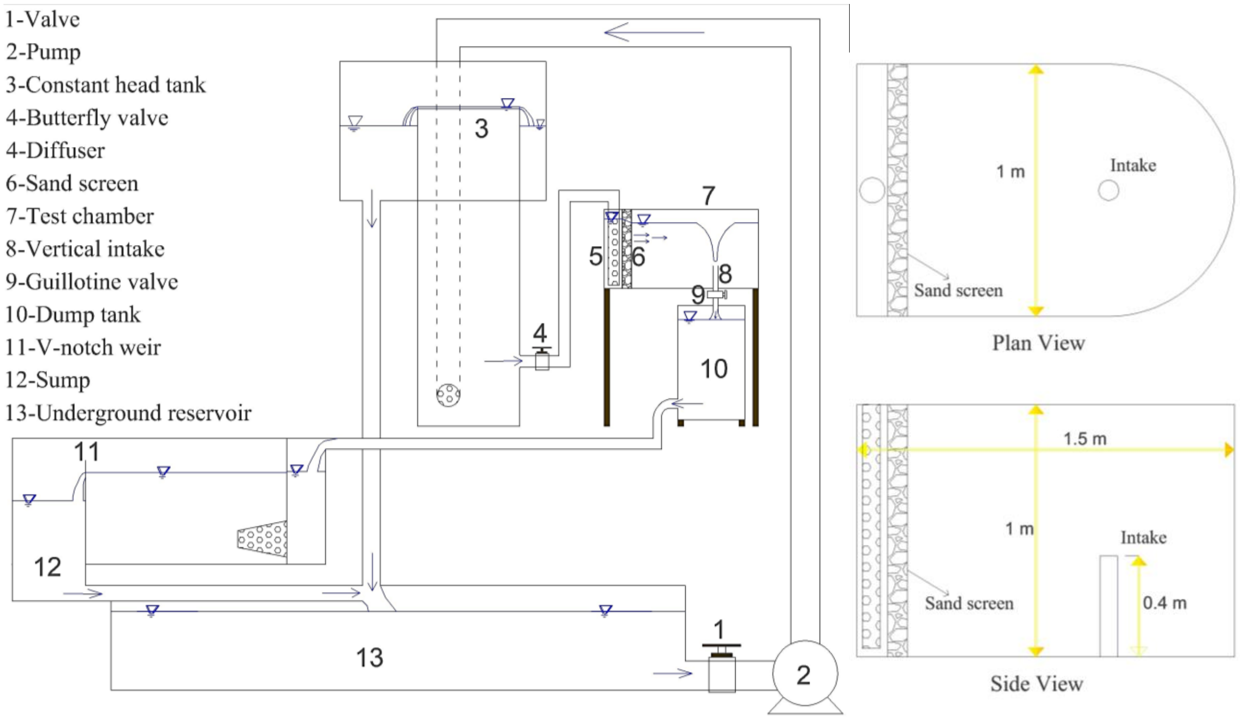

(a) (b)

**Figure 2.** Schematic diagrams (a) side view of the experimental set-up; (b) plan and side views of the test chamber.

A parametric experimental study of the critical submergence at an ogee-shaped intake mouth with and without a cross-vane vortex inhibitor was undertaken and compared to that for a simple pipe intake. The ogee-shaped intake mouth (mounted on the pipe intake) had a height 35 mm as shown in Figure 3 (a). The crossed vane vortex inhibitor was made of perforated vertical plates fixed cross-wise on top of the intake mouth as shown in Figure 3 (b). The vertical plates were made of aluminum whose length, height and perforation diameter varied from 2 to 2.5D, 0.25D to D, and 0.08D to 0.11D, respectively. The perforations were uniformly distributed and resulted in a plate solidity of 0.65 and 0.58 for the perforations of 0.08D and 0.11D, respectively. The experimental parameters tested are shown in Table 2. As the aim of the experiments was to determine the critical submergence, an experimental flow was established with a steady, stable critical vortex (defined as just prior to air-entrainment occurring, VT4). This was achieved by setting the submergence level in the test chamber by controlling the flow at two sections: 1) between the constant head tank and the flume using a butterfly valve to control inflow, 2) under the test chamber downstream of the vertical intake using a guillotine valve to control outflow. For each of the 640 experiments, the discharge rate was set and the submergence adjusted until a steady, stable vortex was produced. Once the vortex was stable for 15 minutes, the hydraulic parameters (discharge and submergence) were recorded. It was considered important for the vortex to be steady to scale the results up to the prototype scale. This differs from previous works in which an unsteady vortex was created under either increasing or decreasing submergence conditions, and whose results may have limited application to prototype vortices (Azarpira et al. 2014, Yang et al. 2014, Monshizadeh et al. 2017, Sarkardeh 2017, Shemsi and Kabiri-Samani 2017). In some of the studies reported in the literature, the conditions used to establish the vortex are not described clearly. For example, Shemsi and Kabiri-Samani (2017) have conducted 400 sets of experiments studying swirling flows using the PK-shaped intake mouth without precisely stating their method of recognizing the critical vortex.

**Table 2.** Test variables.

| Parameters (Unit) | Intake mouth | Discharge rates (*Q*, l/s) | Perforation diameter of vertical meshed vanes ($d_i$) | Dimensions of vertical meshed vanes (*LP***HP*) |
|---|---|---|---|---|
| Values | Simple, Ogee-shaped | 2 – 10 (36 different flow rates) | $d_1$=0.11D, $d_2$= 0.08D | 2D×D/4, 2D×D/2, 2D×D<br>2.5D×D/4, 2.5D×D/2, 2.5D×D |

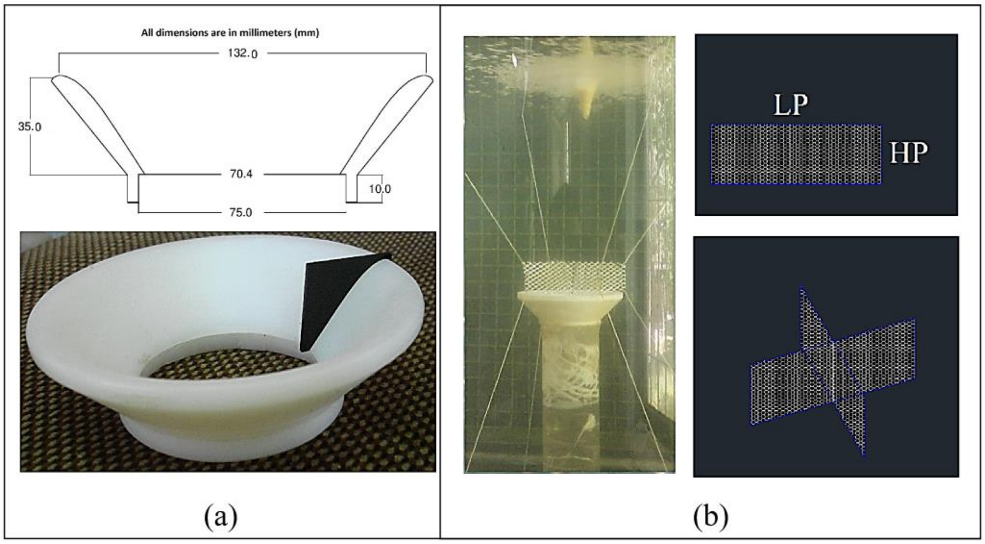

**Figure 3.** (a) Dimensions of ogee-shaped intake mouth; (b) Cross-vanes: vertical perforated plates.

Dimensional analysis can be used to determine the important dimensionless parameters in this experimental study. The vortex formation is determined by the geometry of the intake and the cross-vane vortex inhibitor (*D*, *LP*, *HP*, *d*), the flow conditions (*V*, *g*, *Γ*), and the fluid properties (*ρ*, *μ*, *σ*). The critical submergence, $S_C$, for the present study can therefore be expressed by the following equation:

$$S_C = f_1(\rho, \mu, \sigma, g, V, D, \Gamma, LP, HP, d) \tag{1}$$

Where, $\rho, \mu, \sigma, g, V$ and $\Gamma$ are density, dynamic viscosity and surface tension of water, acceleration due to gravity, discharge velocity and initial circulation. Using Buckingham Π Theorem, a functional equation for the dimensionless critical submergence can be written as:

$$\frac{S_C}{D} = f_2\left(\mathrm{Re} = \frac{\rho V D}{\mu}, \mathrm{Fr} = \frac{V}{\sqrt{gD}}, \mathrm{K} = \frac{\Gamma}{VD}, We = \frac{\rho V^2 D}{\sigma}, \frac{LP}{D}, \frac{HP}{D}, \frac{d}{D}\right) \tag{2}$$

Where *Re*, *Fr*, *K* and *We* are the intake Reynolds number, intake Froude number, intake Kolf number and intake Weber number, respectively. The circulation is dependent on the Froude number, the vortex chamber geometry, and the approach flow conditions (Sarkardeh et al. 2010). The Kolf number depends on the value of the intake discharge, the tank geometry, and the approach geometry (Zaloglu 2014). Based on Sarkardeh et al. (2010) and Zaloglu (2014), Kolf number effects can be omitted because the vortex test tank and intake geometry were constant during the experiments and did not impose any circulation. It should be mentioned that the neglected Kolf Number is related to induced circulation and not the natural circulation of the flow. The Weber number and Reynolds number can be neglected if the experiments are conducted at sufficiently high *Re* and *We* numbers above the criteria identified in Table 3 such that viscosity and surface tension are negligible.

**Table 3.** Range of Weber and Reynolds numbers recommended so that the effect of the surface tension and viscosity can be neglected.

| Researcher | *Re* | *We* |
|---|---|---|
| Daggett & Keulegan (1974) | $Re \geq 3 \times 10^3$ | $We \geq 120$ |
| Anwar et al. (1978) | $Re \geq 10^4$ | $We \geq 100$ |

Neglecting the Kolf, Reynolds and Weber numbers, Equation (2) reduces to:

$$\frac{S_C}{D} = f_3(\mathrm{Fr}, \frac{LP}{D}, \frac{HP}{D}, \frac{d}{D}) \tag{3}$$

## 3. Experimental Results and Analysis

The performance of the ogee-shaped intake with and without the cross-vane vortex inhibitor will be compared to the experiment of the simple pipe intake and three predictive equations (Berge 1966, ASCE 1995, Moller 2013). The experiments were performed at values of Reynolds number and Weber number above 31740 and 158, thus meeting the criteria required to neglect them. Figure 4 presents the results of the simple pipe intake experiments and compares them to the three equations from Table 1 above.

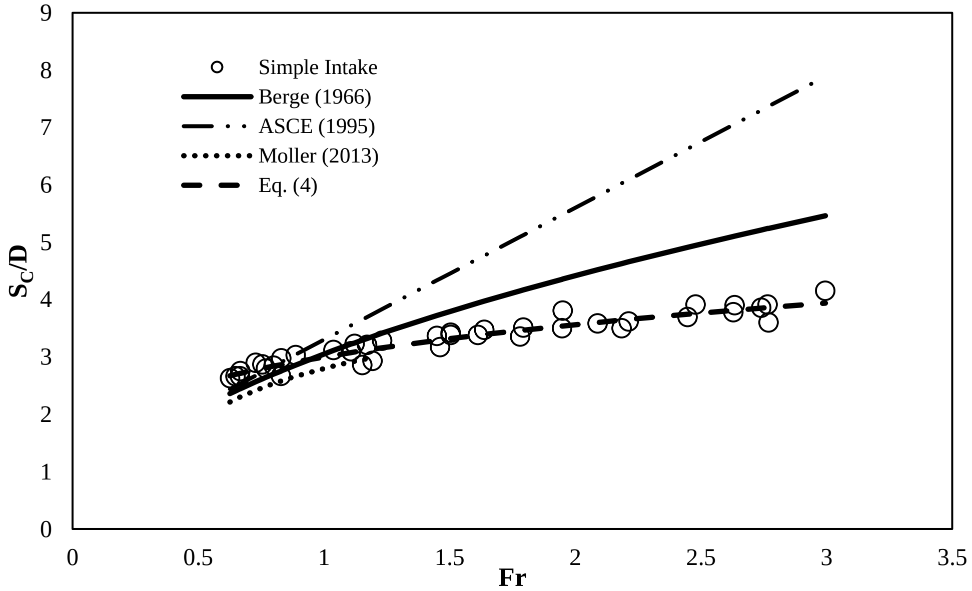

**Figure 4.** Dimensionless submergence versus *Fr* for the simple pipe intake.

The data and predictive equations demonstrate that critical submergence, $S_{C,}$ increases as a function of Froude number, Fr. The differences between the present study and the predictive equations from the literature could be explained by the exact definition of critical submergence (i.e. with or without air-entrainment) and due to differences in intake diameter or tank geometry. A best fit empirical equation for the critical submergence of the current simple intake (with its defined geometry) as a function of Froude number only, having coefficient of determination ($R^2$) of 0.96 is:

$$\frac{S_C}{D} = 3\ \mathrm{Fr}^{0.248} \tag{4}$$

Eq. (4) is valid within the experimental range of $0.62 \leq Fr \leq 3.0$. Experiments over the same range of flow rates with an ogee-shaped intake are presented in Figure 5. The ogee-shaped intake reduces the critical submergence at lower

Froude numbers ($Fr < 1.2$) or equivalently lower discharges. A best fit equation for critical submergence, $S_C$, for an ogee-shaped intake based on Froude number, $Fr$, having a $R^2$ of 0.89 is:

$$\frac{S_C}{D} = 2.67\ \mathrm{Fr}^{0.416} \qquad (5)$$

Eq. (5) is valid within the experimental range of $0.75 \leq Fr \leq 2.6$. A function of performance variable is defined in Eq. (6) to assess the reduction in the critical submergence relative to the base case of the simple intake.

$$f(P)\% = \frac{(\frac{S_C}{D})_i - (\frac{S_C}{D})_n}{(\frac{S_C}{D})_i} \times 100\% \qquad (6)$$

Where $f(P)$ is the function of performance (%) and $(\frac{S_C}{D})_i$ is the normalized critical submergence of the simple intake and $(\frac{S_C}{D})_n$ is the normalized critical submergence being compared. The average performance of an ogee-shape intake over the Froude number range of 0.62 to 3.0 is 5.5% (i.e. a reduction of critical submergence of 5.5%) as shown in Figure 5.

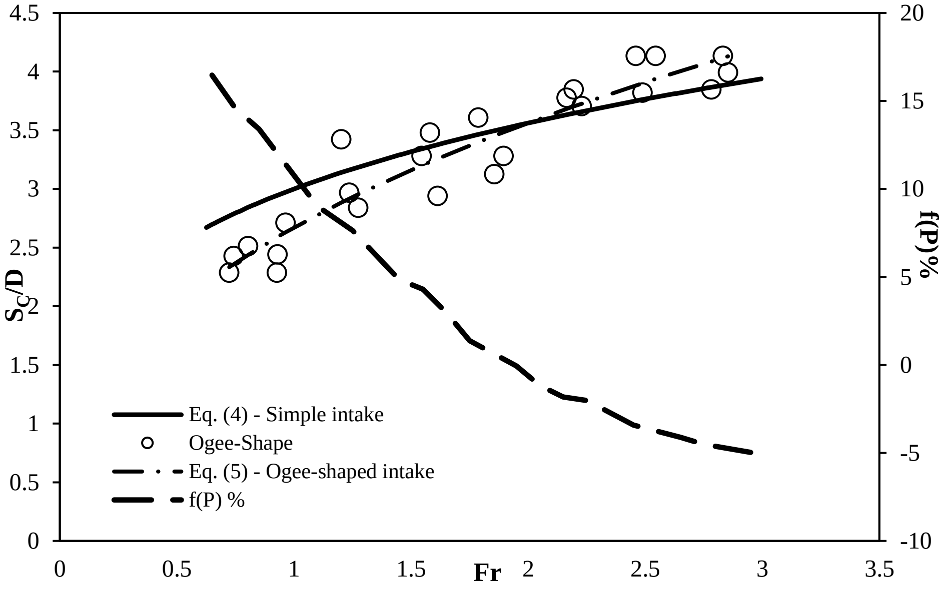

**Figure 5.** Dimensionless critical submergence and functional performance of an Ogee-shaped intake versus $Fr$ compared to the simple intake.

A cross-vane vortex inhibitor with a range of lengths, heights and perforation diameters was investigated to determine its effect on the critical submergence of the ogee-shaped intake. The variation of the critical submergence as a function of Froude number with lengths of 2D or 2.5D and heights of D/4, D/2, and D with a perforation diameter of 0.11D is shown in Figure 6. Except at the highest Froude numbers ($Fr > 2.5$), the cross-vane vortex inhibitor reduced the critical submergence values. Figure 7 presents the results for the same geometrical variation of the vortex inhibitor but with perforation diameters of 0.08D. Both figures indicate that and ogee-shaped intake with cross-vane vortex inhibitor also results in increasing critical submergence at increasing Froude number. When compared to the simple intake, the critical submergence is increasingly reduced as the Froude number decreases below 2.5. The best fit equations for subsets of data are provided in Table 4. Modifying the geometry of the cross-vane vortex inhibitor results in little change to the general trend as shown in these equations, the functional performance values for each case at three different Froude number ranges, and averaged over all Froude numbers; this is shown in Figure 8.

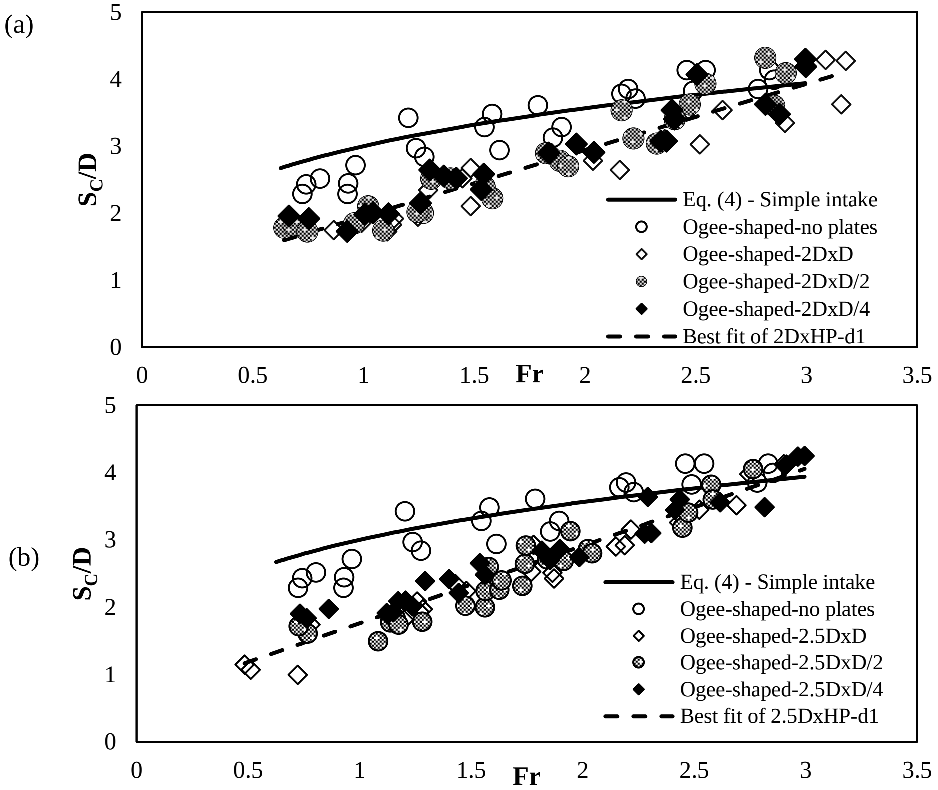

**Figure 6.** Variation of $S_C/D$ versus *Fr* for different vertical meshed plates ($d_i$ =0.11D); (a): *LP*=2D, (b): *LP*=2.5D.

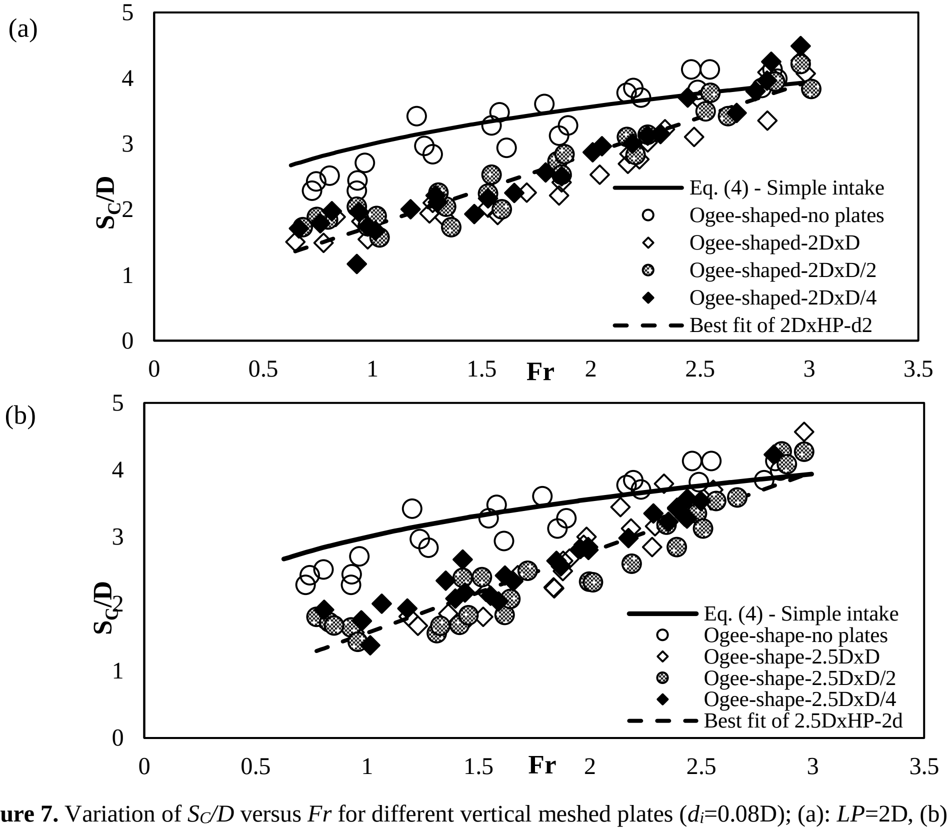

**Figure 7.** Variation of $S_C/D$ versus *Fr* for different vertical meshed plates ($d_i$=0.08D); (a): *LP*=2D, (b): *LP*=2.5D.

**Table 4.** Best fit equations for subsets of data.

| Type of vertical meshed plates | Best fit equation | $R_2$ |
|---|---|---|
| (2D×D)-$d_i$=0.11D | $\frac{S_C}{D} = 0.99\ \mathrm{Fr} + 0.96$ | 0.9 |
| (2D×D/2)-$d_i$=0.11D | | |
| (2D×D/4)-$d_i$=0.11D | | |
| (2.5D×D)-$d_i$=0.11D | $\frac{S_C}{D} = 1.15\ \mathrm{Fr} + 0.61$ | 0.93 |
| (2.5D×D/2)-$d_i$=0.11D | | |
| (2.5D×D/4)-$d_i$=0.11D | | |
| (2D×D)-$d_i$=0.08D | $\frac{S_C}{D} = 1.1\ \mathrm{Fr} + 0.65$ | 0.9 |
| (2D×D/2)-$d_i$=0.08D | | |
| (2D×D/4)-$d_i$=0.08D | | |
| (2.5D×D)-$d_i$=0.08D | $\frac{S_C}{D} = 1.2\ \mathrm{Fr} + 0.37$ | 0.87 |
| (2.5D×D/2)-$d_i$=0.08D | | |
| (2.5D×D/4)-$d_i$=0.08D | | |

A best fit empirical equation for the critical submergence of the ogee-shaped intake for all the subsets of data as a function of Froude number only, having coefficient of determination ($R^2$) of 0.89, is:

$$\frac{S_C}{D} = 1.11\ \mathrm{Fr} + 0.66 \qquad (7)$$

Eq. (7) and all those of Table 4 are valid within the experimental range of $0.5 \leq Fr \leq 3.2$.

The vortex inhibitor is effective at reducing the critical submergence, particularly at lower Froude numbers, as it reduces the critical submergence by 39%, 32% and 8% for the Froude number ranges of 0 to 1, 1 to 2, and 2 to 3, respectively, as shown in Figure 8.

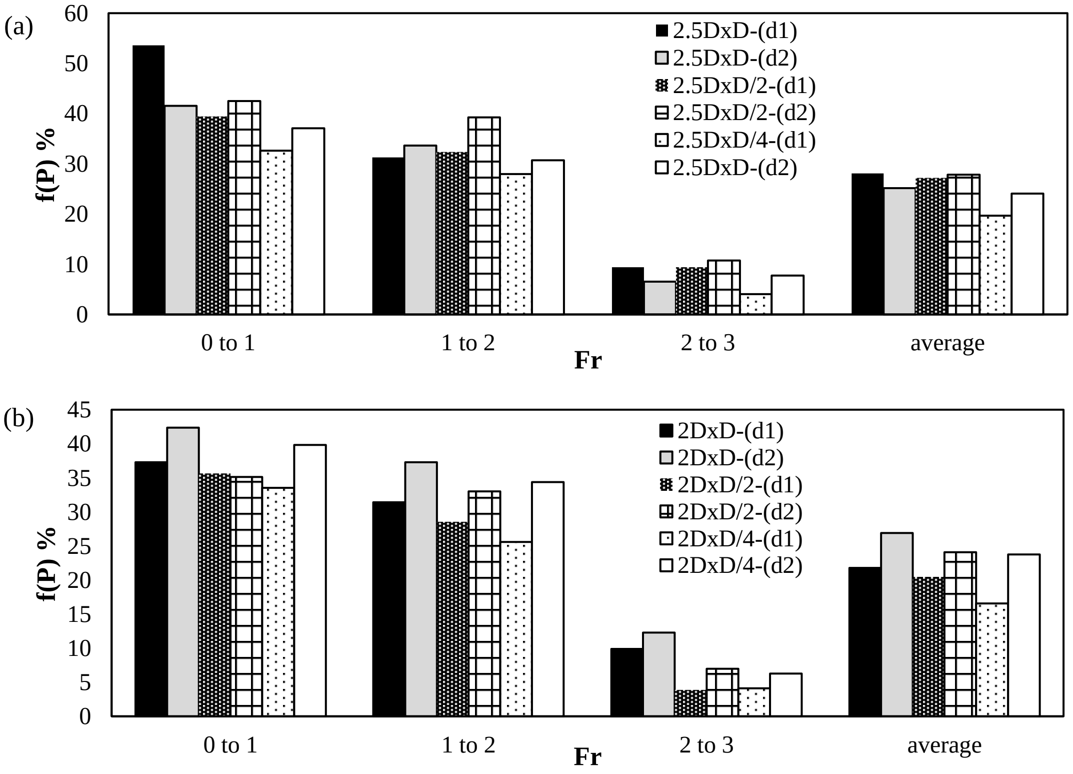

**Figure 8.** Functional performance, *f(P)*, versus *Fr*; (a): *LP*=2.5D, (b): *LP*=2D.

The effect of varying the geometry of the cross-vane vortex inhibitor is of the same magnitude as the experimental variation. The average and variation in the data presented as subsets of data holding one vortex inhibitor parameter constant is presented in Figure 9. Note that the standard deviation parameter, S.D., within a subset of data is of the same magnitude as the variation between subsets of data. However, all geometric variation of the cross-vane vortex inhibitor reduces the critical submergence greater than 20%.

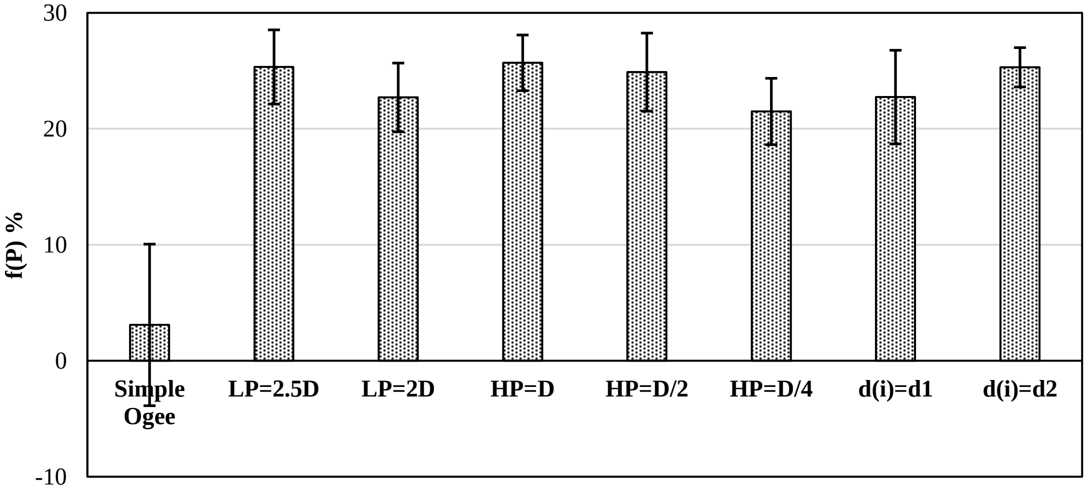

**Figure 9.** Average *f(P)* for all the anti-vortex plates combined to the ogee intake versus $Fr$ (Underlining S.D.).

The limitations of use for Eq. (6) are for the Froude number range of $0.5 \leq Fr \leq 3.2$ and for the following ranges of the geometrical parameters of the cross-vane vortex inhibitor: $0.25 \leq \frac{HP}{D} \leq 1,\ 2 \leq \frac{LP}{D} \leq 2.5,\ 0.08 \leq \frac{d}{D} \leq 0.11$. Normalized critical submergence values were calculated using Eq. (7) and plotted versus those observed in Figure 10.

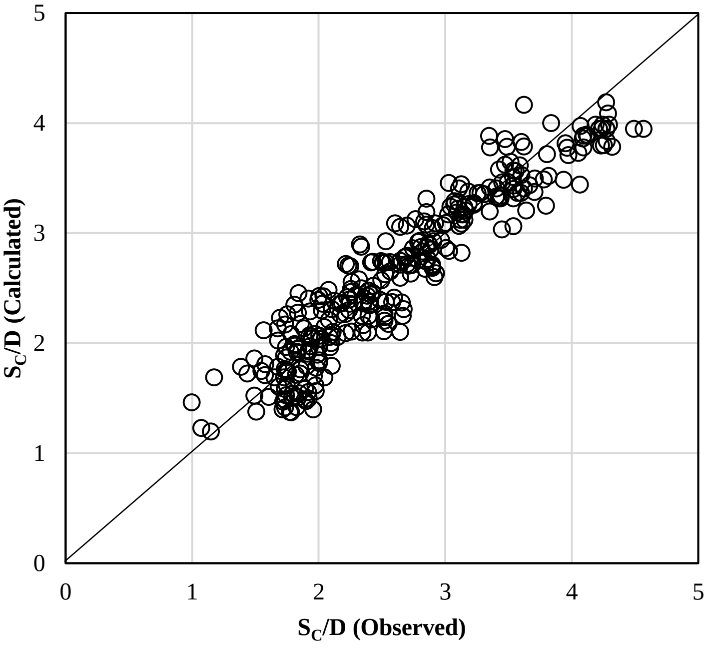

**Figure 10.** Calculated critical submergence values versus observed counterparts.

## 4. Conclusions

A parametric study was undertaken to investigate the effectiveness of a cross-vane vortex inhibitor on a vertical intake with an ogee-shaped intake mouth in a uniform approach flow. The scaling criteria by past authors indicated that at sufficiently high Reynolds and Weber numbers, the effects of viscosity and surface tension can be neglected. This criterion was met in the experimental set up. Using dimensional analysis resulted in an equation for critical submergence as a function of Froude number and three dimensionless parameters describing the geometry of the cross-vane vortex inhibitor (length, height and perforation diameter of the vanes). A parametric study of the critical submergence of a simple pipe intake, the ogee-shaped intake, and the ogee-shaped intake with vortex inhibitor was undertaken for Froude number range of $0.5 \leq Fr \leq 3.2$ and for the following ranges of the geometrical parameters of the cross-vane vortex inhibitor: $0.25 \leq \frac{HP}{D} \leq 1$, $2 \leq \frac{LP}{D} \leq 2.5$, $0.08 \leq \frac{d}{D} \leq 0.11$. For all intakes, the critical submergence increased with increasing Froude number. The ogee-shaped intake resulted in a moderate reduction in critical submergence compared to the simple intake at lower Froude number (with increased reduction with decreasing Froude number). The cross-vane vortex inhibitor was effective at reducing the critical submergence for Froude numbers less than 2.5 and was increasingly effective as Froude number reduced. The critical submergence was insensitive to the range of the tested geometric parameters of the cross-vanes. An empirical equation was developed to predict critical submergence as a function of Froude number for an ogee-shaped intake with a cross-vane vortex inhibitor having the $R^2$ value of 0.89.

## 5. References

Anwar, H.O., Weller, J.A., and Amphlett, M.B. (1978). “Similarity of free-vortex at horizontal intake.” *Journal of Hydraulic Research*, 16(2), 95-105.

Anwar, H.O., Amphlett, M.B. (1980). “Vortices at vertically inverted intake.” *Journal of Hydraulic Research*. 18(2), 123–134.

American Society of Civil Engineers (ASCE). (1995). Guidelines for Design of Intakes for Hydroelectric Plants. Committee on Hydropower Intakes of the Energy Division, New York, USA.

Azarpira, M., Sarkardeh, H., Tavakkol, S., Roshan, R., and Bakhshi, H. (2014). “Vortices in dam reservoir: A case study of Karun III dam.” *Journal of the Indian Academy of Sciences*, 39(5): 1201-1209.

Berge, J.P. (1966). “Enquête sur la formation de vortex et autres anomalies d’écoulement dans une enceinte avec ou sans surface libre.” *Houille Blanche* .21(1), 13–27.

Borghei, S.M., and Kabiri-Samani, A.R. (2003). “Critical submergence of vertical intakes using anti-vortex plates.” *Proceedings of the 6th International Conference in Civil Engineering*, IUT, Isfahan, Iran, 7,59-66.

Borghei S.M., and Kabiri-Samani, A.R. (2010). “Effect of anti-vortex plates on critical submergence at a vertical intake.” *Scientia Iranica*. 17(2), 89-95.

Chen, Y., Chao, W.U., Mao, Y.E., and Xiao-Ming, J.U. (2007). “Hydraulic characteristics of vertical vortex at hydraulic intakes.” *Journal of Hydrodynamics*, Volume 19(2), 143-149.

Cristofano, L., Nobili, M., and Caruso, G. (2014). “Experimental study on unstable free surface vortices and gas entrainment onset conditions.” *Experimental Thermal and Fluid Science*, 52, 221-229.

Daggett, L.L., and Keulegan. G.H. (1974). “Similitude conditions in free-surface vortex formation.” *Journal of Hydraulic Engineering*, ASCE 100(11), 1565-1580.

Gao, X., Zhang, H., Liu, L., Sun, B., and Tian, Y. (2018). “Numerical investigation of flow in a vertical pipe inlet/outlet with a horizontal anti-vortex plate: effect of diversion orifices height and divergence angle.” *Engineering Applications of Computational Fluid Mechanics*, 12(1), 182-194.

Gulliver, J.S., Rindels, A.J., Lindblom, K.C. (1986). “Designing intakes to avoid free-surface vortices.” *International Water Power and Dam Construction*, 38(9), 24–28.

Hashid, M., Hussain, A., and Ahmad, Z. (2015). “Discharge characteristics of lateral circular intakes in open channel flow.” *Flow Measurement and Instrumentation*, 46, 87-92.

Hecker, G.E. (1987). Fundamentals of vortex intake flow. Conclusions. In: Knauss, J, editor. Swirling flow problems at intakes. IAHR hydraulic structures design manual. Rotterdam: Balkema, [chapters 2 and 8].

Hite, J.E., and Mih, W.C. (1994). “Velocity of air-core vortices at hydraulic intakes.” *Journal of Hydraulic Engineering*, ASCE, 120(3), 284-297.

Jain, A.K., Rangaraju, K.G., and Garde, R.J. (1978). "Vortex formation at vertical pipe intakes." *Journal of the Hydraulics Division*. ASCE, 104(10), 1429–1448.

Levi, L. (1991). "Vortices in hydraulics." *Journal of Hydraulic Engineering*, 117(4), 399-413.

Li, H., Chen, H., Zheng, M.A., and Zhou, Y. (2008). "Experimental and numerical investigation of free surface vortex." *Journal of Hydrodynamics*. 20(4), 485-491.

Mih, W.C. (1990) "Analysis of fine particle concentrations in a combined vortex." *Journal of Hydraulic Research*, 28(3), 392-396.

Möller, G. (2013). Vortex-Induced Air Entrainment Rate at Intakes. PhD Dissertation, ETH Zurich, Switzerland.

Monshizadeh, M., Tahershamsi, A., Rahimzadeh, H., and Sarkardeh, H. (2017). "Comparison between hydraulic and structural based anti-vortex methods at intakes." *The European Physical Journal Plus*, 132(8), 329.

Naderi, V., Farsadizadeh, D., Hosseinzadeh-Dalir, A., and Arvanaghi, H. (2013). "Experimental study of bell-mouth intakes on discharge coefficient." *Journal of Civil Engineering and Urbanism*, 3(6), 368-371.

Naderi, V., Farsadizadeh, D., Hosseinzadeh-Dalir, A., and Arvanaghi, H. (2014). "Effect of using vertical plates on vertical intake on discharge coefficient." *Arabian Journal for Science and Engineering*. 39(12), 8627-8633.

Odgaard, A.J. (1986). "Free-surface air core vortex." *Journal of Hydraulic Engineering*. ASCE, 112(7), 610-620.

Rankine, W.J.M. (1858). A Manual of Applied Mechanics, Charles Griffin, London.

Reddy, Y.R., and Pickford, J.A. (1972). "Vortices at intakes in conventional sumps." *International Water Power and Dam Construction*, 24(3), 108–109.

Rindels, A.J., and Gulliver, J.S. (1983). An experimental study of critical submergence to avoid free-surface vortices at vertical intakes. Technical report, St. Anthony Falls Hydraulic Laboratory, University of Minnesota, Minneapolis, US.

Rosenhead, L. (1930). "The spread of vorticity in the wake behind a cylinder." *Proceedings of the Royal Society of London*. Series A, 129(809), 115-135.

Rudolf, P., and Klas, R. (2015). "Numerical simulation of pump-intake vortices." *Proceedings of Experimental Fluid Mechanics 2014: The European Physical Journal Web of Conferences.* Cesky Krumlov, Czech Republic, 92,02077.

Sarkardeh, H. (2017). "Minimum reservoir water level in hydropower dams." *Chinese Journal of Mechanical Engineering*, 30(4), 1017-1024.

Sarkardeh, H., Zarrati, A.R., and Roshan, R. (2010). "Effect of intake head wall and trash rack on vortices." *Journal of Hydraulic Research*, 48(1), 108-112.

Shemshi, R., and Kabiri-Samani, A. (2017) "Swirling flow at vertical shaft spillways with circular piano-key inlets." *Journal of Hydraulic Research*, 55(2), 248-258.

Suerich-Gulick, F., Gaskin, S.J., Villeneuve, M., and Parkinson, E. (2014). "Free surface intake vortices: theoretical model and measurements." *Journal of Hydraulic Research*, 52(4), 502-512.

Sun, H., and Liu, Y. (2015). "Theoretical and experimental study on the vortex at hydraulic intakes." *Journal of Hydraulic Research*, 53(6), 787-796.

Tastan, K. (2016). "Critical submergence for isolated and dual rectangular intakes." *Journal of the Indian Academy of Sciences*, 41(4), 425–433.

Tastan, K., and Yıldırım, N. (2010). "Effects of dimensionless parameters on air-entraining vortices." *Journal of Hydraulic Research*. 48(1), 57–64.

Yıldırım, N., and Kocabas, F. (1995). "Critical submergence for intakes in open channel flow." *Journal of Hydraulic Engineering*, 121(12), 900–905.

Wang, Y.K., Jiang, C.B., and Liang, D.F. (2011a). "Comparison between empirical formulae of intake vortices." *Journal of Hydraulic Research*, 49(1), 113–116.

Wang, Y.K., Jiang, C.B., and Liang, D.F. (2011b). "Study on theoretical submergence of surface vortices and the design of anti-vortex intakes." *Science China Technological Sciences.54(4), 799–804.*

Yang, J., Liu, T., Bottacin-Busolin, A., and Lin, C. (2014). "Effects of intake-entrance profiles on free-surface vortices." *Journal of Hydraulic Research*, 52(4), 523-531.

Zaloglu, C. (2014). Formation of Air-Entraining Vortices at Horizontal Water Intakes. M.Sc. Dissertation, Middle East Technical University, Ankara, Turkey.